ACS OMEGA

Open Access

http://pubs.acs.org/journal/acsodf

Article

Effect of Benzoic Acid on Biogenic Gas Production with Different Rank Coals and the Fluorescence Spectra Characteristic of Produced Organic Products

Guoqin Wei, Dangyu Song, Huan He,* Xianbo Su, Daping Xia, Yunbo Li, and Yu Qiao

Cite This: *ACS Omega* 2025, 10, 16169−16183

Read Online

ACCESS | Metrics & More | Article Recommendations

ABSTRACT: Biogas production was conducted using samples from different coal beds and laboratory-domesticated microbes to investigate the effect of the addition of benzoic acid on biogas production. Furthermore, the response properties of produced organic substances at different gas production stages were analyzed with ultraviolet−visible (UV−Vis) spectroscopy and three-dimensional fluorescence spectroscopy. The results showed that adding benzoic acid significantly enhanced the microbial gas production with different rank coals. Obvious spectroscopic differences were observed in the gas production effects and liquid-phase composition across varying rank coals. The UV−vis spectroscopy findings indicated that soluble organic matter gradually increased in molecular weight during gas production, leading to increased aromatization and an increase in aromatic ring substituents with hydrogen and oxygen functional groups. Fluorescence spectroscopy revealed changes in protein-like substances during gas production, indicating the involvement of humic acid-like substances from coal in microbial gas production. The results of the fluorescence index supported the biological origin of humic acid during the gas production process. Benzoic acid augmentation promoted biogas production in different coal grades, and distinct differences were observed in the organic spectral properties during gas production, suggesting that the metabolic pathways of the same microbes acting on different coal grades vary.

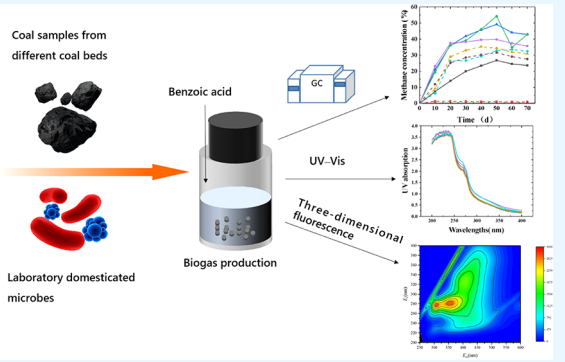

1. INTRODUCTION

Coal biogas production is an active process driven by a series of microorganisms that degrade, transform, and generate methane from the organic matter present in coal under anaerobic conditions.[1] Middle- and low-rank coals, such as lignite and long-flame coal, exhibit characteristics of high moisture, ash, volatile content, low calorific value, and a high content of humic acid. Due to these properties, the direct combustion of these coals is less beneficial. Nonetheless, their organic material, containing oxygen and side-chain functional groups, offers a suitable substrate for the production of microbial biogenic gas.[2] Dissolved organic matter (DOM) within middle- and low-rank coals possesses various reactive groups, including hydroxyl, carboxyl, amino, and aromatic rings. It displays high mobility and reactivity and plays a crucial role by being transferred into the liquid phase during biogas generation mediated by microorganisms.[3,4] The exact mechanism of methane formation from microbial degradation of coal under anaerobic conditions remains inconclusive. However, the classical "four-stage" theory of anaerobic fermentation, involving hydrolysis, acidification, hydrogen−acetic acid production, and methanogenesis, has gained support from most researchers.[5,6] Numerous researchers have analyzed the composition and changes in intermediate products during biogas formation to gain insight into the potential metabolic mechanisms of anaerobic degradation. For instance, Omar et al.[7] observed significant variations in the concentration of alkanes and palmitic acid in the C22−C36 range during the biogas formation process of sub-bituminous coals. Chen et al.[8] reported the importance of volatile fatty acids and long-chain alkanes in coal biogenic gas formation. Highlighting the significance of volatile organic acids (C2 ± C7), Liu et al.[9] characterized over 30 intermediates involved in coal biogenic gas production. Coal biogas production is affected by various factors such as microbial species, temperature, pH, coal maturity, and nutritional substrates. Robbins et al.[10] observed that the lower coal maturity enhanced biogas production, correlating with higher concentrations of low-molecular-weight acids (C2 ± C7 abundance), which was closely associated with changes in the abundance of specific

Received: October 29, 2024
Revised: April 3, 2025
Accepted: April 7, 2025
Published: April 15, 2025

Table 1. Results of Coal Proximate Analysis and Coal Ultimate Analysis[a]

Samples	Mad (%)	Aad (%)	Vdaf (%)	FCad (%)	Cdaf (%)	Hdaf (%)	Odaf (%)	Sdaf (%)	Ndaf (%)	Calorific value (MJ kg^{-1})
S	1.32	20.20	13.70	69.60	92.60	3.75	1.11	1.30	1.24	28.92
X	2.31	12.74	22.72	67.87	87.90	3.13	2.40	0.81	1.03	26.09
N	17.52	21.53	48.79	31.20	71.59	5.54	20.65	0.94	1.35	20.67

[a]ad (air-dry) base, daf (dry ash free) base.

microbial taxa. These variations were closely associated with changes in the abundance of special microorganisms capable of degrading these acids and alcohols. Jones et al.[11] demonstrated that the addition of nutrients or microorganisms to coal seams lacking coalbed methane production could stimulate gas production. It has been suggested that the addition of small-molecule nutrient substrates, such as micronutrients favorable for the growth of methanogenic bacteria, significantly enhances the gas production capacity.[12] Notably, benzoic acid, a common degradation product of humic acid found in lignite, has been reported to improve the yield of biogas with lignite when added to culture media.[13] However, the precise mechanisms by which benzoic acid affects coal biogas production and the accumulated intermediates still remain unclear.

The technique of three-dimensional fluorescence (3D fluorescence) is frequently employed for the qualitative and quantitative analysis of organic compounds due to its strong selectivity, rapid analytical speed, easy sample pretreatment, and nondestruction of the sample structure.[14,15] Furthermore, the fluorescence spectrum analysis can be used to determine the distribution, composition, and source of DOM transferred to the liquid phase during coal degradation based on the peak position, number, and fluorescence intensity.[16] In order to explore the initial connection between the generation of biogas and the changes in organic matter and coal rank differences, biogas production simulation experiments were conducted using coals of different ranks in two types of culture media: one with the addition of benzoic acid and another without. The aim of these experiments was to further investigate the effects of different coal types and addition of benzoic acid on gas formation and changes in organic matter. By offering essential data, it hopes to underline the mechanism of the biogas formation process, thus making a valuable contribution to the field of biogenic coalbed methane (CBM) production.

2. MATERIALS AND METHODS

2.1. Methanogenic Microorganisms and Culture Media. The methane-producing microorganisms used in these experiments were previously cultivated and domesticated in our earlier research.[17] These microorganisms exhibited impressive capabilities in the degradation of coal and the production of gas. For the cultivation of these microorganisms, two modified media were employed. The first medium, designated as medium I (add benzoic acid group), had the following composition per liter: benzoic acid: 0.2 g, yeast extract: 1.5 g, K_2HPO_4: 2.9 g, KH_2PO_4: 1.5 g, NH_4Cl: 1.8 g, $MgCl_2$: 0.4 g, and 1 mL each of trace elements and vitamins. The second medium, medium II (no benzoic acid group), shared the same composition as medium I, except that it did not include benzoic acid. To meet the nutritional requirements of the microorganisms, the trace elements and vitamins in the media were prepared according to established literature recommendations.[18]

2.2. Coal Sample Collection and Analysis. The three coal samples used in this study were obtained from the no. 3 coal seam of Shanxi Jincheng Sihe Mine (sample no. S), the no. 4 coal seam of Shanxi Taiyuan Xishan Mine (sample no. X), and the no. 5 coal seam of Shenhua Nortel Shengli Open-pit Coal Mine in Inner Mongolia (sample no. N). Upon transport to the laboratory, the fresh coal samples were promptly crushed and sifted. Subsequently, they were dried to a constant weight at room temperature and subjected to coal proximate analysis (GB/T 30732-2014) and coal ultimate analysis (GB/T 31391-2015) following national standards. The results are shown in Table 1. The coal proximate analysis results indicated that Sihe coal (S) is anthracite, Xishan coal (X) is bituminous, and Inner Mongolia coal (N) is lignite.

2.3. Biogas Production Experiments with Different Rank Coals. Coal samples from three different coal beds were utilized as substrates for the biogas production experiments. A specific experimental protocol was adopted: 9 g of coal was combined with 225 mL of either medium I or medium II in a 500 mL anaerobic bottle. The mixture was sterilized at 120 °C for 20 min before cooling to room temperature. Following this, 100 μg/L vitamins and 0.25 g/L cysteine were added to an anaerobic bottle in the anaerobic glovebox (DG1000, DWS, UK). Next, 45 mL of microbial broth was inoculated, and the bottles were sealed with butyl rubber plugs and aluminum caps. The experiment was conducted at a constant temperature of 35 °C for 70 days.

The experimental design included six groups: S1 (Sihe coal + benzoic acid), S2 (Sihe coal), X1 (Xishan coal + benzoic acid), X2 (Xishan coal), N1 (Inner Mongolia coal + benzoic acid), and N2 (Inner Mongolia coal). Each group differed based on the type of coal and whether or not benzoic acid was present in the medium. Two additional control groups (CK1 and CK2) were also created by inoculating microorganisms without coal samples. In the first group, benzoic acid was added, while the medium in the second group remained free of benzoic acid. All experiments were performed in triplicate, and the results were averaged. Gas samples were collected at regular intervals throughout the incubation period and analyzed using gas chromatography (7890A, Agilent, USA) to determine the composition of the biogas produced during the anaerobic incubation. The chromatographic analysis conditions are described in the literature.[19,20]

2.4. UV−Vis and Fluorescence 3D Spectroscopy of Dissolved Organic Matter Formed during Biogenic Gas Production from Different Rank Coals. During the biological gas production process, liquid samples (10 mL each) were taken from the anaerobic flask every 10 days and subjected to ultraviolet and fluorescence 3D spectroscopy. The samples were filtered through a 0.45 μm microporous filter membrane before being frozen at −20 °C for preservation and analysis. Using a UV−Vis spectrophotometer (UV-4820), we measured the UV absorption spectra of the samples within the range of 200 nm−400 nm. This allowed us to calculate various ratios, including E250/E365, E240/E420, E253/E203, and E253/E220, which provided information on the molecular structure of the dissolved organic matter.[21] We also used a

https://doi.org/10.1021/acsomega.4c09883
ACS Omega 2025, 10, 16169−16183

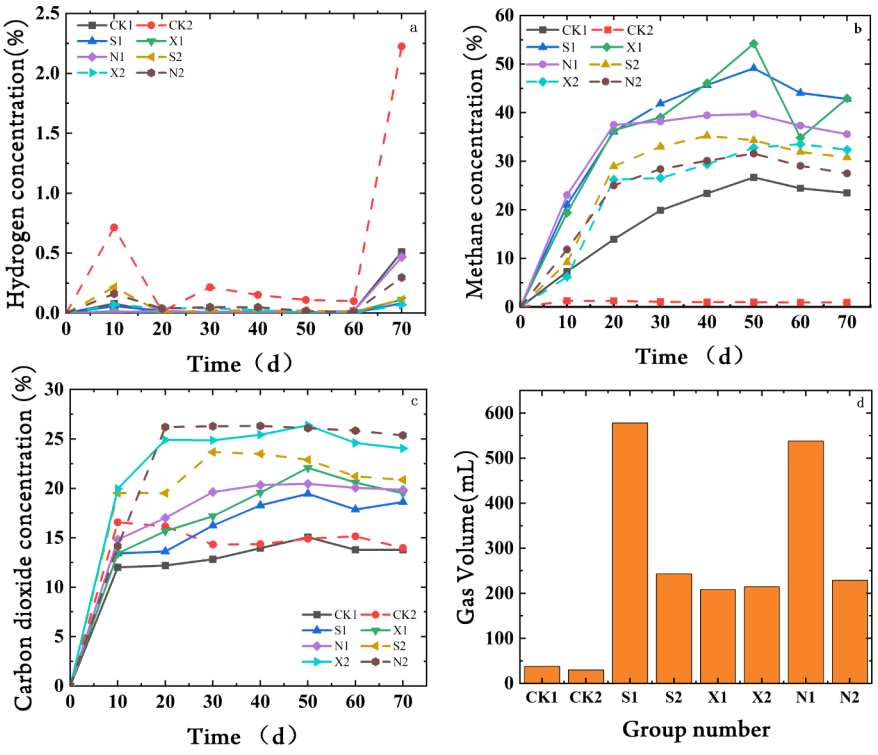

Figure 1. Variation curves of gas components and contents in the biogenic gas production process of coal of different ranks: (a) H_2, (b) CH_4, (c) CO_2, and (d) total gas production.

fluorescence spectrophotometer (HI-TACHIF-7000) to measure the 3D fluorescence spectra of the samples. The analyzing conditions included a 150 W hernia lamp as the light source, a photomultiplier tube (PMT) set at 700 V, and diffraction grating monochromators for both excitation and emission. The slit width was maintained at 10 nm, the scanning speed was 1200 nm/min, and the wavelength ranges for both excitation and emission were 200 nm−400 and 240 nm−600 nm, respectively. The step size was set to 2 and 5 nm for excitation and emission, respectively. The response time was automatic, and ultrapure water served as a blank to correct for Raman scattering from the water. Data were analyzed and processed using Origin software (Version 9.1, OriginLab Corp.)

2.5. Calculation of the Fluorescence Integral Using the Fluorescence Area Integration Method. The 3D fluorescence spectra were segmented into five regions based on excitation/emission wavelength combinations.[22] These substances corresponded to each region as shown in the reference.[23] The fluorescence intensity at specific wavelengths depends on the concentration of fluorophores present. MATLAB 2022 software was used to perform the region integration (FRI) calculation, which computes the specific fluorescence region integration volume (Φ_i), representing the cumulative fluorescence intensity of organic matter with similar properties. The formula for calculating Φ_i is as follows:

$$\Phi_i = \int_{ex}\int_{ex} I_{\lambda ex,\lambda em} d\lambda_{ex} d\lambda_{ex} \quad (1)$$

However, since the areas of the segmented regions were unequal, the interpretation of the volume integral for each region across the entire data set was influenced by the differing areas of the regions. Therefore, it is proposed that this effect can be mitigated by normalizing the area of each region separately.

$$MF_i = \frac{\sum_{i=1}^{5} S_i}{S_i} \quad (2)$$

Here, S_i represents the area of region i and MFi is termed the multiplicative factor. The volume integral of the corrected region i is denoted as

$$\Phi_i = \Phi_i \times MF_i \quad (3)$$

The fluorescence integral for each region was calculated using the MATLAB 2022 program.

2.6. Fluorescence Index Calculation. The fluorescence index (FI) is defined as the ratio of the spectral intensity at an excitation wavelength of 370 nm with an emission wavelength in the range of 450 nm−500 nm. FI was utilized for the assessment of humus.[24]

3. RESULTS AND DISCUSSION

3.1. Changes in Gas Components and Contents during Biogas Production from Different Rank Coals. Figure 1 shows biogas production from three types of coal. The analysis of total gas production and its production trend reveals a distinct cycle consisting of three stages: a rapid period (5−20 days), a peak period (20−50 days), and a stabilization period (50−75 days). Notably, the highest gas occurs in the early stages, followed by a subsequent decrease, particularly in the later stages (Figure 1d). Similar studies have shown that during rapid periods of characterization by high organic carbon content in nutrient sources, there was an ensured availability of small organic molecules consumed by microorganisms.[25] The consistently observed stabilization period in all studies examining coal bioconversion to methane can be attributed to the depletion of nutrients and the initial decline in coal dissolution. The inhibition of gas production was due to the generation of inhibitory compounds, such as volatile fatty acids

https://doi.org/10.1021/acsomega.4c09883
ACS Omega 2025, 10, 16169−16183

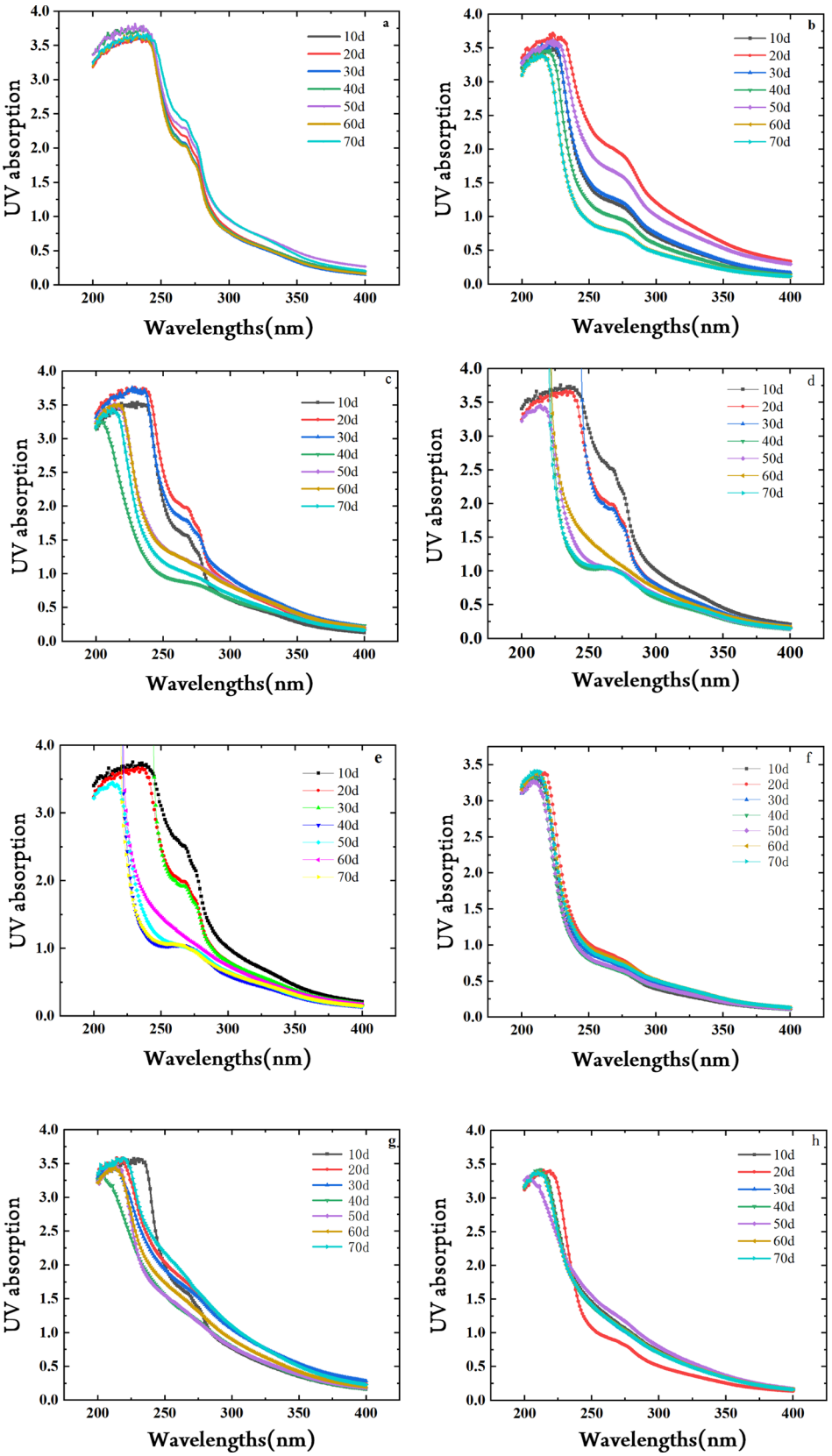

Figure 2. Variation curves of UV spectra in the process of coal biogas production from different rank coals: (a) CK1, (b) CK2, (c) S1, (d) S2, (e) X1, (f) X2, (g) N1, and (h) N2.

or heavy metals. The inhibition of gas production may be caused by the generation of inhibitory compounds, such as volatile fatty acids or heavy metals.[26]

The concentration of hydrogen (H_2) remains relatively stable throughout the entire incubation period. However, the blank control group (CK2) exhibits the highest H_2 content during the

https://doi.org/10.1021/acsomega.4c09883
ACS Omega 2025, 10, 16169−16183

initial incubation period (0−10 days), reaching 1.1% (Figure 1). Furthermore, all samples exhibited a decreasing trend in H_2 production from 0 to 20 days, followed by a plateau from 20 to 60 days and a gradual increase after 60 days (Figure 1a). This can be attributed to the early-stage microorganism primarily utilizing small molecular compounds from the culture medium and coal to produce H_2. As the available small molecular compounds became limited, the H_2 content did not exhibit a significant rapid increase. Moreover, it is hypothesized that methanogens utilize H_2 produced in the reaction system to synthesize the final product CH_4, thus consuming H_2. It is suggested that the methanogens in the entire reaction system predominantly follow the acetic acid or methyl nutrient pathway.[27] After 60 days, the macromolecular compounds in the coal were utilized by the previous fermentation and hydrogen−acetic acid-producing microorganisms to synthesize more H_2. The slow decrease in the amount of methane produced during this period further indicated that the methanogens in the system were not predominantly of the hydrogen-nutrient type. This further suggests that the addition of benzoic acid may influence the metabolic pathway of gas production. Peak gas production has been significantly prolonged, and it increased significantly following the addition of benzoic acid, indicating that the microbial community in the fermentation group with benzoic acid was more active. This enhancement in microbial activity increased the capability of small molecular acids to convert into biomethane, leading to increased gas production.[28]

Analysis of changes in the carbon dioxide (CO_2) content revealed an increasing trend until day 35, after which it stabilizes. Moreover, the overall CO_2 production in the group without benzoic acid (S2, X2, N2, and CK2) exceeds that of the benzoic acid-added group (S1, X1, N1, and CK1) (Figure 1b). Interestingly, the group with N2 exhibited an obvious decreasing trend in CO_2 production on the 10th day. This indicated that the Inner Mongolia coal (N) utilized CO_2 to synthesize CH_4 using methanogenic microorganisms during the early stage of biogas production. Methanogenic organisms use CO_2 in large quantities to synthesize CH_4. The amount of CH_4 produced by all three rank coals in both media significantly exceeded that of the control group (Figure 1c). Generally, peak methane production occurred around the 50th day with the following monitored methane contents: S1 (49.95%), X1 (56.09%), N1 (39.77%), S2 (34.11%), X2 (33.58%), and N2 (31.92%). There are primarily two ways to produce biological methane: the acetic acid and the methyl nutrient pathway. The change in CO_2 content during biological coal gasification reflected the pathway of biological methane production.[29] Previous research has demonstrated a positive correlation between methane and CO_2 in the acetic acid pathway. Alternatively, when these two gas components exhibited a negative correlation, it was attributable to the methyl nutrient pathway.[30] Moreover, considering the impact of gas production in both media, the methane production concentration in the benzoic acid-added group (S1, X1, N1, and CK1) significantly outperformed that of the group without benzoic acid (S2, X2, N2, and CK2). This suggests that benzoic acid can improve microbial methane production in different coal types.

In general, the coal samples from the Sihe and Xishan regions exhibited higher gas production compared with those from the Inner Mongolia. This contradicts prior studies suggesting that low-rank coals with higher ash and volatile matter are more suitable for microbial coal gas production. The findings of some studies indicated that lower-rank coals exhibited a higher degree of biodegradability due to the presence of a higher concentration of aliphatic hydrocarbons and heteroatoms, which were more susceptible to microbial degradation.[31] Some studies have shown that methane production from the microbial degradation of coal was negatively correlated with an increase in coal rank. This conclusion was attributable to the higher aromatic content of high-rank coal.[10] However, some other scholars believe that there was no correlation between methane production from microbially degraded coal and the rank of coal and that the activity of microbial sources was the main factor affecting biogenic gas generation.[32] The findings from certain CBM well production site monitoring exercises indicated that coal with a higher rank exhibited a higher biomethane production rate, despite the absence of a direct correlation between methane generation and coal rank.[33]

Notably, the addition of benzoic acid obviously increased total gas production in Sihe and Xishan coal samples, indicating that benzoic acid stimulated microbial growth, replenished depleted nutrients, and augmented gas production, especially in the gas production process from intermediate- and high-rank coals. This was attributable to the migration mechanisms and rates of organic matter between the solid and liquid phases. The medium−high rank coals have more developed pore structure characteristics and interconnected pores and fractures compared to low rank coal, which enhances the migration rate of organic matter between the solid and liquid phases, making it easier for organic matter to migrate between the solid and liquid phases. Adding benzoic acid affected this mechanism and modified the gas production pathway. Preliminary research indicated that benzoic acid served as an intermediate product during the anaerobic metabolism of aromatic compounds, degrading acetic acid (an intermediate containing carbon). This degradation stimulated the methanogenic system to prioritize the metabolic pathway of CH_3COOH decomposition into CH_4, resulting in increased CH_4 production.[34]

3.2. UV−Vis Analysis of Solution Components in the Biogas Production Process from Different Rank Coals.

Figure 2 depicts the UV−Vis spectra of the obtained liquid-phase samples during the biogenic gas production process from different rank coals. These spectra exhibited significant changes, with maximum absorption peaks occurring near 220 and 280 nm for both the blank control group and the experimental group. Notably, the absorption peaks of the blank control group (CK1 and CK2) exhibited a pattern of initial decrease, followed by an increase and then a subsequent decrease. In contrast, the absorption peaks of the experimental groups (S, X, and N) continued to decrease during the gas production cycle. Particularly noteworthy were the pronounced changes observed within the 0−3 days and 9−20 days periods. The absorption peaks at 220 and 280 nm corresponded to the $n-\pi$ conjugation and $\pi-\pi$ conjugation of aromatic compounds, respectively. The shoulder peaks at 220 and 280 nm in the blank control group (CK1 and CK2) remained relatively stable as the gas production time increased. Conversely, the shoulder peaks at 280 nm in the experimental groups (S, X, and N) disappeared entirely and formed a continuous absorption band at 250 nm−300 nm. Shoulder-like peaks at 280 nm in the experimental groups continued to weaken from 0 to 10 days, indicating an enhanced organization level of DOM in the liquid phase. After 30 days, the decrease in the shoulder-like peaks gradually reduced, with some individual groups exhibiting recovery. In the blank control group CK1, the shoulder peaks consistently remained at a certain level, indicating that the microorganisms preferred the utilization of

https://doi.org/10.1021/acsomega.4c09883
ACS Omega 2025, 10, 16169−16183

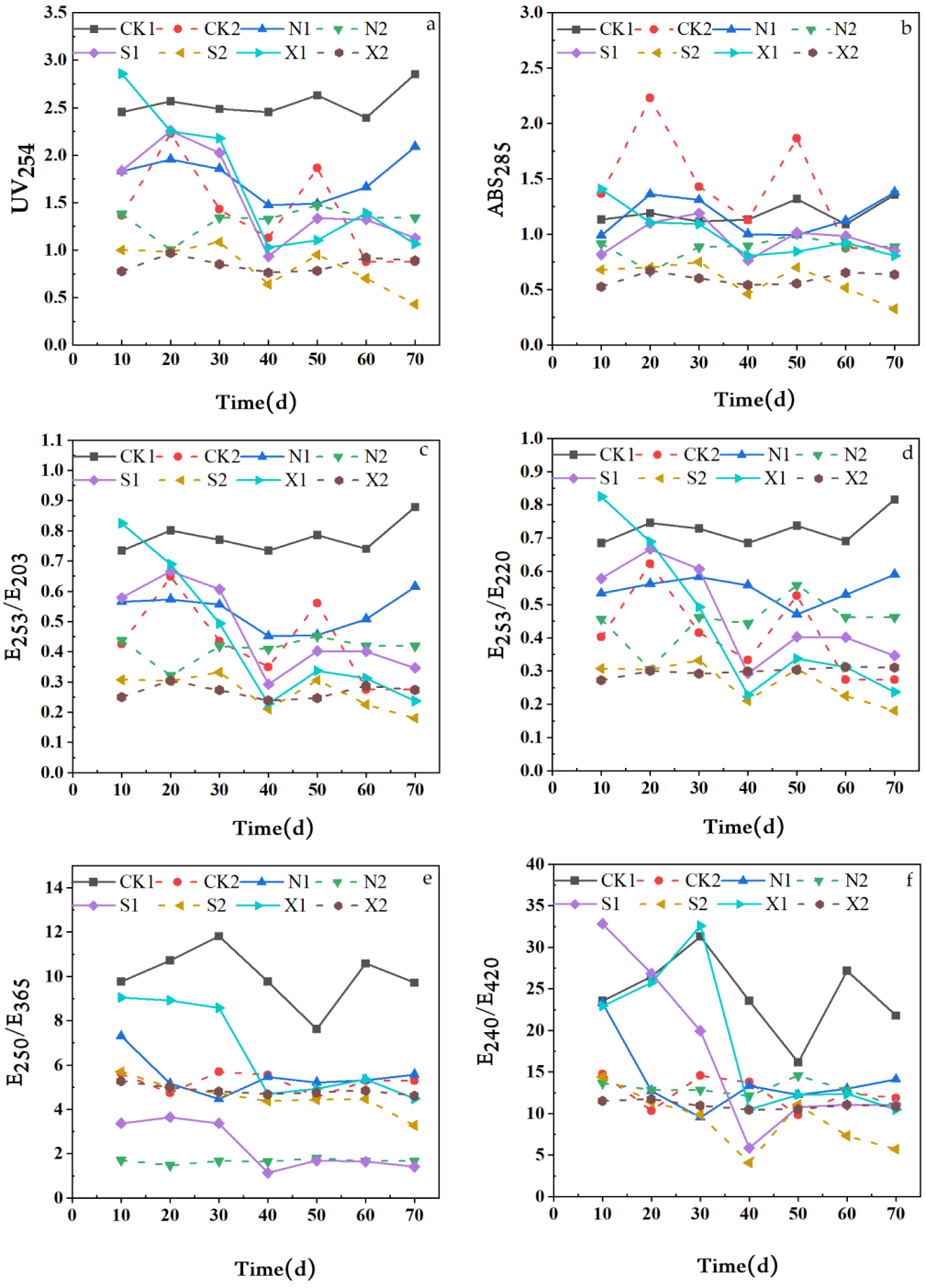

Figure 3. Variation curves of UV characteristic parameters for coal biogas production from different rank coals: (a) UV254, (b) ABS285, (c) E253/E203, (d) E253/E220, (e) E250/E365, and (f) E240/E420.

easily accessible substances in the nutrient solution, while their ability to utilize aromatic substances was relatively weak. In the benzoic acid-added test group (S1, X1, and N1), the shoulder peaks of Sihe (S1) and the Xishan area (X1) exhibited a significant downward trend, while the shoulder peaks of the benzoic acid group in the Inner Mongolia area (N1) showed a relatively insignificant decrease. This result indicated that coal from the Sihe and Xishan regions exhibited more favorable metabolic processes for methane production within the microbial gas production system. Consequently, it is possible to engineer conditions to create a more conducive environment for microbial activity, thereby promoting microbial degradation of coal and enhancing gas production.[35] Some studies have shown that benzoic acid facilitated the removal of CO_2 to generate catechol, with subsequent decomposition to yield pyruvate and acetyl-CoA.[36] These intermediates participated in the tricarboxylic acid cycle, enhancing the activity of methanogens, stimulating methane synthesis, and ultimately improving the performance of fermentation gas production.[37]

The UV absorption spectrum at 254 nm mainly reflected changes in compounds with unsaturated C−C bonds, particularly aromatic compounds, which displayed greater resistance to degradation. In the CK1 group, a slight shift in UV254 was observed throughout the gas formation process.

https://doi.org/10.1021/acsomega.4c09883
ACS Omega 2025, 10, 16169−16183

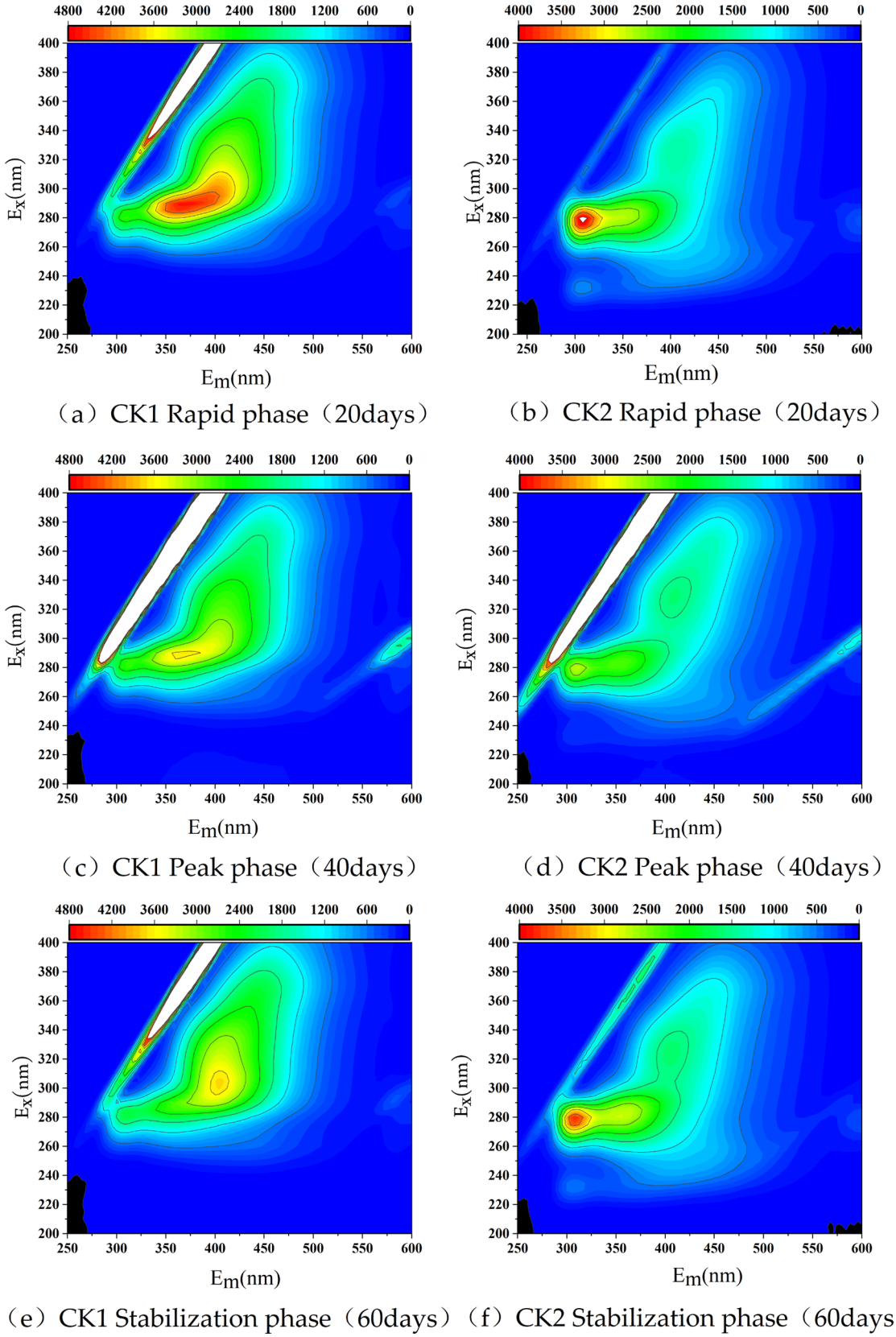

Figure 4. Analysis of fluorescence spectral changes during biological gas production in CK1 and CK2 groups: (a) CK1 rapid phase (20 days), (b) CK2 rapid phase (20 days), (c) CK1 peak period (40 days), (d) CK2 peak period (40 days), (e) CK1 stabilization period (60 days), and (f) CK2 stabilization period (60 days).

Conversely, the experimental group (S, X, and N) exhibited a slight shift during the initial 30 days, followed by a rapid decrease from 30−40 days, reaching a stabilized state afterward. This phenomenon indicated that microorganisms in the blank

https://doi.org/10.1021/acsomega.4c09883
ACS Omega 2025, 10, 16169−16183

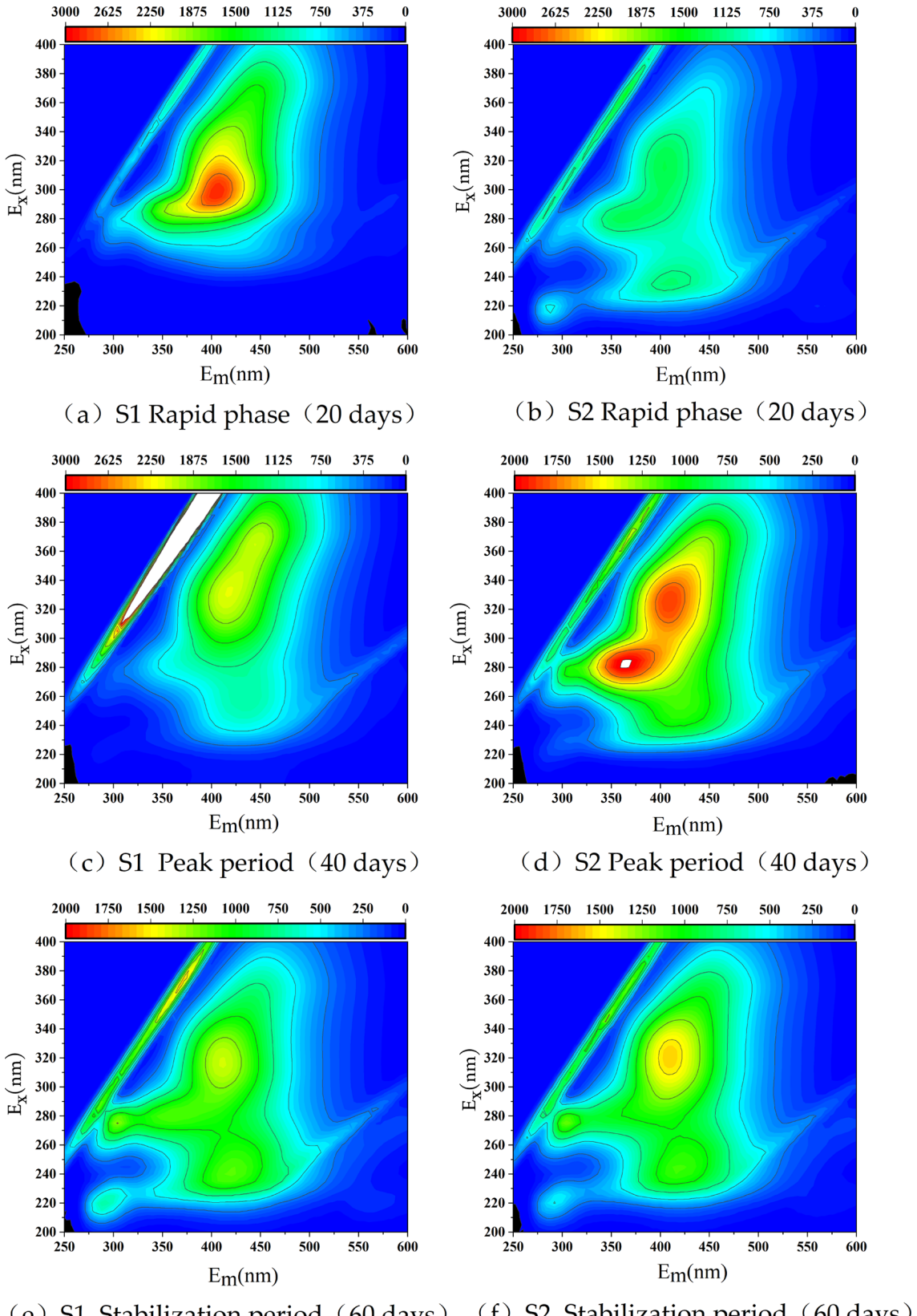

Figure 5. Analysis of fluorescence spectral changes during biological gas production in groups S1 and S2: (a) S1 rapid phase (20 days), (b) S2 rapid phase (20 days), (c) S1 peak period (40 days), (d) S2 peak period (40 days), (e) S1 stabilization period (60 days), and (f) S2 stabilization period (60 days).

control group were unable to effectively utilize unsaturated compounds, such as aromatics, which were more difficult to decompose in the medium. In the experimental group, despite rapid gas production, a slight shift in the aromatic compounds

https://doi.org/10.1021/acsomega.4c09883
ACS Omega 2025, 10, 16169−16183

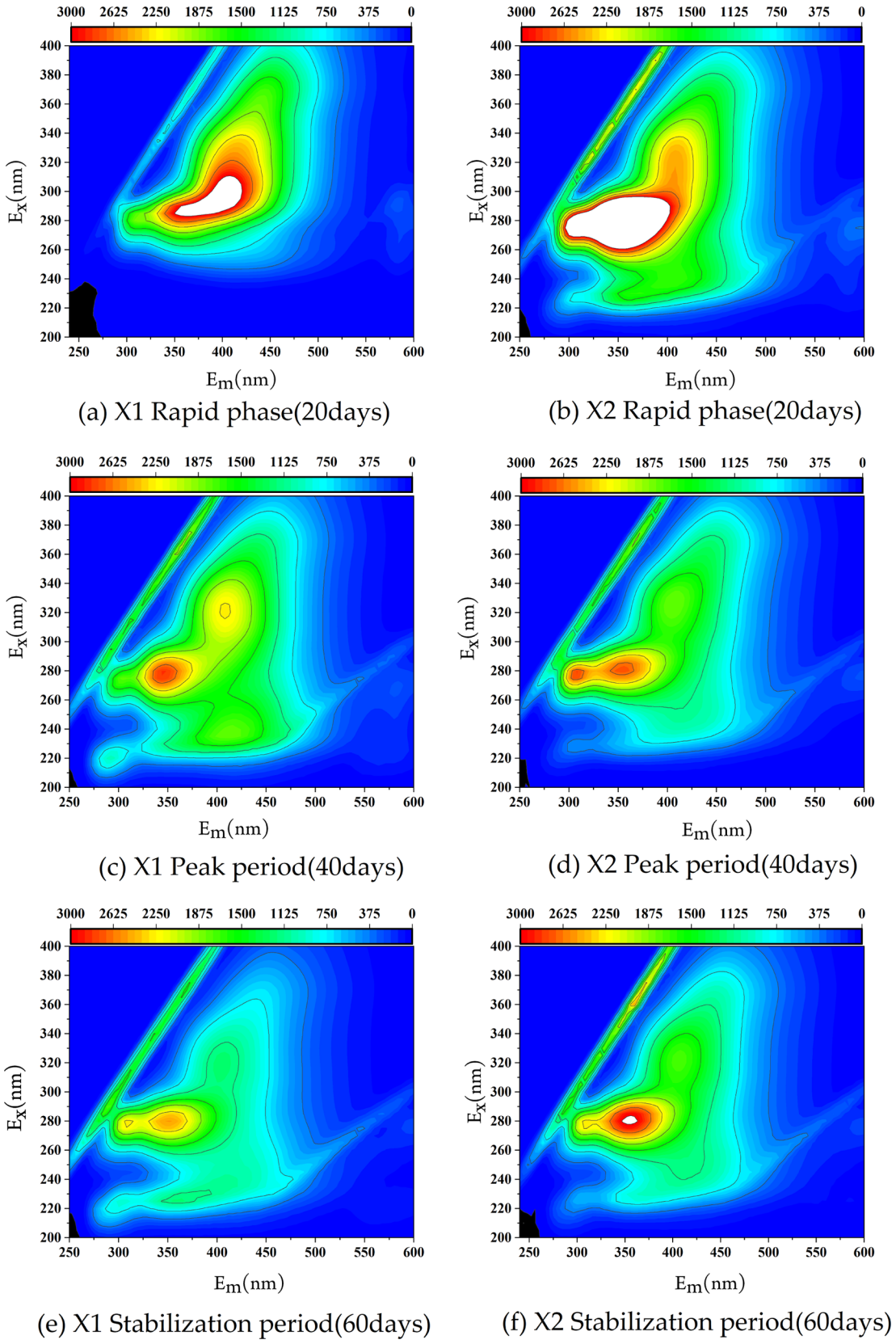

Figure 6. Analysis of fluorescence spectral changes during biological gas production in groups X1 and X2: (a) X1 rapid phase (20 days), (b) X2 rapid phase (20 days), (c) X1 peak period (40 days), (d) X2 peak period (40 days), (e) X1 stabilization period (60 days), and (f) X2 stabilization period (60 days).

was observed within 10 days. This indicated that microbes initially prioritize the utilization of easily decomposable substances in the coal and the medium, including tiny molecular compounds and readily available nutrients, before the formation

https://doi.org/10.1021/acsomega.4c09883
ACS Omega 2025, 10, 16169−16183

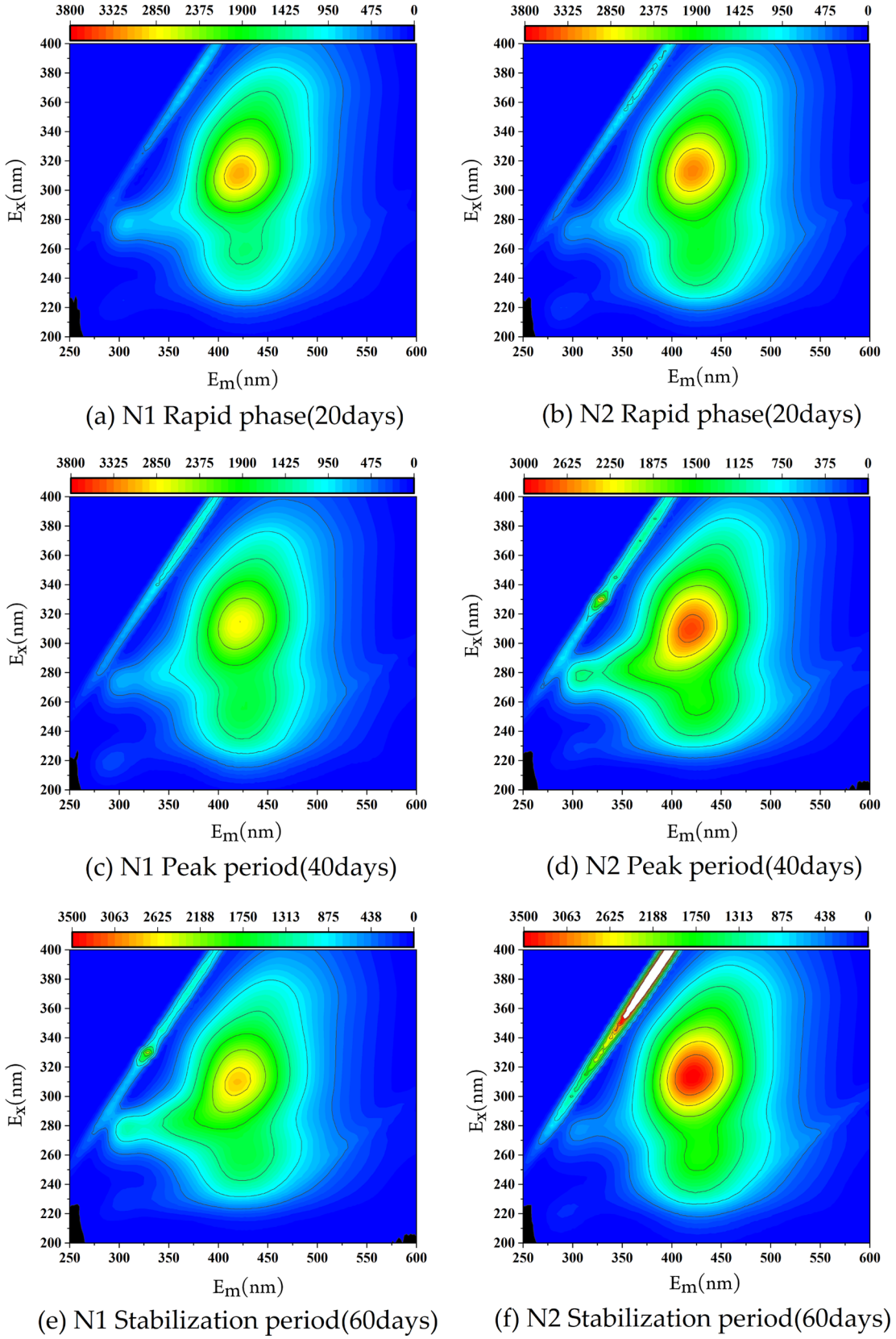

Figure 7. Analysis of fluorescence spectral changes during biological gas production in groups N1 and N2: (a) N1 rapid phase (20 days), (b) N2 rapid phase (20 days), (c) N1 peak period (40 days), (d) N2 peak period (40 days), (e) N1 stabilization period (60 days), and (f) N2 stabilization period (60 days).

of aromatic substances.[38] Furthermore, with the continuous consumption of various organic matter, the UV absorption of

https://doi.org/10.1021/acsomega.4c09883
ACS Omega 2025, 10, 16169−16183

the CK2 group exhibited an increasing trend from 10 to 20 days, a decreasing trend from 20 to 40 days, and an increasing trend from 40 to 50 days before attaining stability.

The UV absorption properties of organic substances at 285 nm, termed ABS285, were used to characterize the degree of aromaticity. A higher ABS285 value indicated higher aromaticity and a greater aromaticity (Figure 3b). The figure clearly demonstrates that the CK1 group displayed a relatively smooth shift in the aromatic group, while the experimental group consistently exhibited a lower aromatic content compared to the control group. This suggests the continuous depletion of the aromatic group in the experimental group. Specifically, N1 and S1 showed an initial upward trend for the first 20 days, followed by a gradual decline. However, X1 exhibited a gradual decrease, with a higher aromatic content during the rapid gas production period compared with the later stages. This result indicated that aromatic groups were continuously depleted during the gas formation process. Furthermore, N1 and S1 exhibited a increasing and then decreasing trend during the first 20 days, while X1 gradually decreased, indicating that the available nutrients differ across various coal types. Hence, the gradual decrease in gas production corresponds to the declining aromatic content, highlighting its role in the gas production process.

The analysis of solution components during the fungal degradation of lignite via UV−Vis spectroscopy was investigated in previous studies, yielding findings consistent with our research. Thus, a characteristic absorption peak at 250 nm−300 nm was attributable to the aromatic rings.[39] As the degradation time increased, the absorption value at 290 nm exhibited a pattern of initial increase followed by stabilization, corresponding to the alteration in extracellular protein content.[40] These findings highlighted the significant role of extracellular proteins in coal degradation, confirming further exploration of our research. In future work, we will use techniques such as petrographic analysis and liquid chromatography−mass spectrometry to further clarify the relationship between organic matter changes and microbial communities in different coal ranks during the formation of biogas.

The parameters E253/E203 and E253/E220 elucidated the degree of aromatic ring substitution and the types of substituents present. A decrease in these values indicated a higher prevalence of substituent fatty chains on the aromatic ring, while an increase indicated a rise in the number of carbonyl, carboxyl, hydroxyl, and ester substituents on the aromatic ring. Figure 3 demonstrates that the ratio in the control group remained relatively stable during the gas production process. Contrastingly, the experimental group experienced an initial increase in these ratios for the first 20 days, followed by stabilization after a drastic decrease between 20 and 40 days. This observation indicated that during the stage of rapid gas production (5−15 days), the aliphatic chain substituting the aromatic ring was continuously degraded into carbonyl, carboxyl, hydroxyl, and ester groups. The final results indicated an increase in oxygen-containing reactive functional groups within the coal due to microbial activity.

The UV−Vis absorbance ratio at specific wavelengths, such as E250 and E365, reflected the molecular weight status of the DOM, with larger ratios indicating smaller molecular weights. Similarly, E240 and E420 characterize the degree of agglomeration and the molecular weight size, with higher values indicating less agglomeration and smaller molecular weight. Generally, the molecular weight of the experimental group was generally lower than that of the control group. Specifically, in Figure 3d, it can be observed that the molecular weights of the control group were smaller than those of the experimental group during the gas formation cycle. The molecular weights of soluble organic matter in the experimental group exhibited a trend of initial increase followed by stabilization, with the most pronounced changes occurring during the first 30 days in group I. This indicated that larger molecules continuously enter the liquid phase and serve as substrates for gas production, which microorganisms utilize to produce gas. This phenomenon was consistent with reports in the literature that molecular weight variability occurs during the gas-producing phase.

The results of UV analysis showed that the shoulder peaks of the samples in the group with added benzoic acid from the Sihe and Xishan regions exhibited a significant decreasing trend, while the shoulder peaks of the Inner Mongolia group decreased insignificantly. This trend corresponded to the gas production results, further confirming that the laboratory strain was more suitable for the Sihe and Xishan coal samples. The system was more conducive to gas production, especially after the addition of benzoic acid. It is hypothesized that the degradable matter conducive to gas production migrates from the solid to the liquid phase. Some biodegradable substances, such as small-molecule fatty acids, can be used as nutrients by microorganisms directly, while larger molecules require more enzymes and steps for degradation, thus creating a more suitable environment for microbial growth. This contradicts previous findings, suggesting that low-rank coals are more favorable for biogas production. Therefore, further exploration is warranted to investigate the adaptability of the microbial community to different coal types and their effects on gas formation under different system conditions.

3.3. Fluorescence Spectroscopy During Biogenic Gas Production from Different Rank Coals. Figures 4−7 show the 3D fluorescence spectra of coal biogas production from different rank coals. Diagonal lines in the figures denote Raman and Rayleigh scattering peaks, which did not affect the analysis of the experimental results. The fluorescence spectra revealed a distinct characteristic absorption peak (EX = 280 nm, Em = 300 nm) in the control group, corresponding to tyrosine-like substances. As gas generation progressed, the experimental group exhibited characteristic absorption peaks attributable to humic acid with a shift in the fluorescence peak position. The intensity and number of fluorescence peaks differ obviously among coal types over the same periods, with the most notable variations occurring during the rapid gas production period. For example, during the peak gas production period of 10−20 days in the Sihe group S2, a coal sample exhibited a change from 1 to 2 fluorescence peaks, characterized by a humic acid-like absorption peak. The intensity of these fluorescence peaks distinctly decreased. The reduced intensity of the fluorescence peak indicated that humic acid-like substances played an essential role in the gas production period. Variations in characteristic peaks and absorption peaks among different coal samples indicated that differences in coal quality components played an important role in gas production.[41] The humic acids exhibited a slight variation during the rapid gas production stage. A continuous increase in concentration was observed during the stable gas production stage. Studies have shown that monocyclic and polycyclic volatile organic compounds, along with soluble carbon, were more susceptible to bioconversion into methane.[42] Other research groups have shown that monocyclic aromatic compounds extracted from lignin and coal facilitate methano-

https://doi.org/10.1021/acsomega.4c09883
ACS Omega 2025, 10, 16169−16183

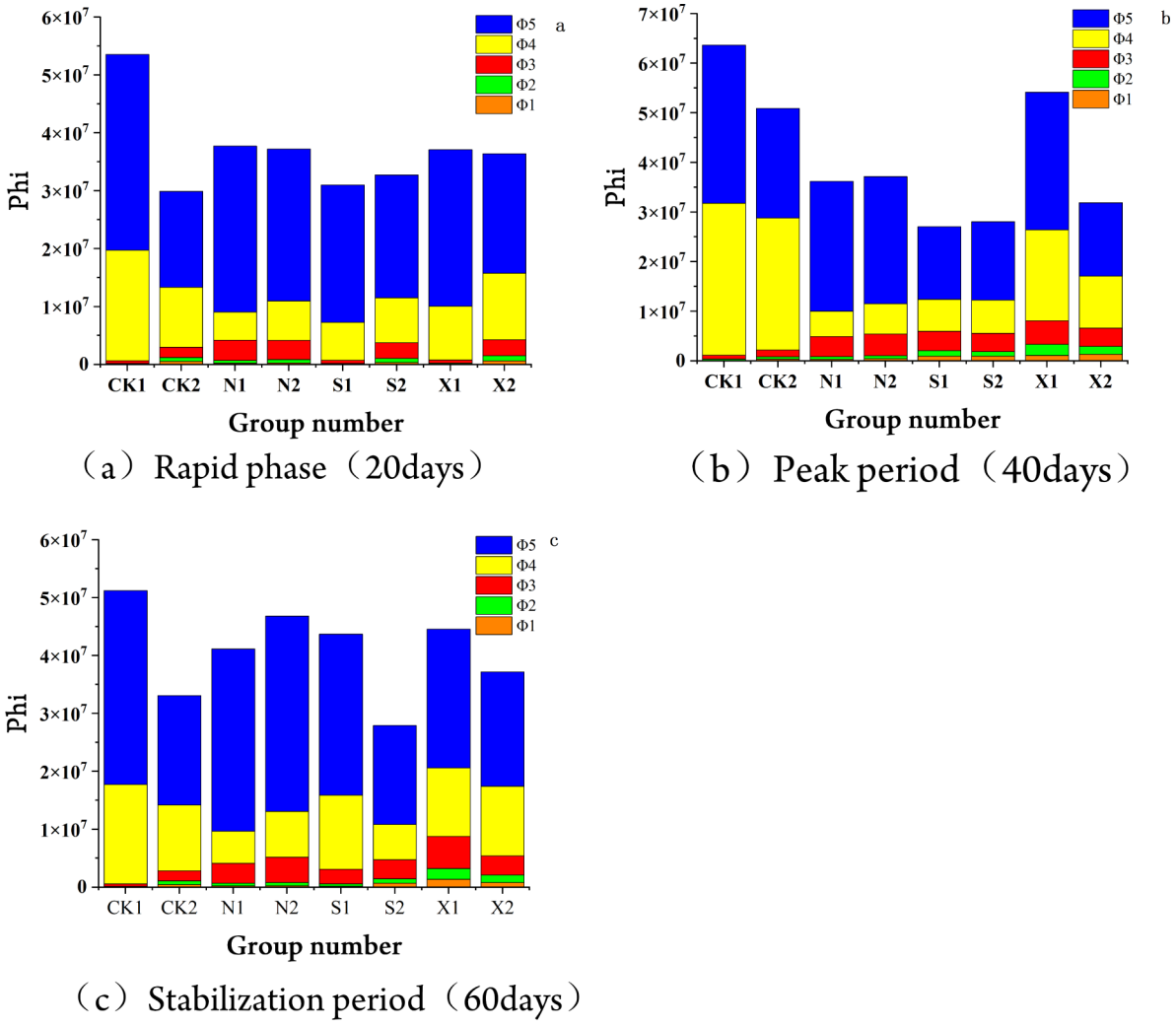

Figure 8. Comparison of fluorescence peak areas in each region of different coal samples during gas production: (a) rapid phase (20 days), (b) peak period (40 days), and (c) stabilization period (60 days).

genic activity. This study conducted further research to explore the relationship between the coal type and microbial methane generation.

Furthermore, comparing the benzoic acid-added group (S1, X1, N1, and CK1) with the no benzoic acid group (S2, X2, N2, and CK2), the former exhibited protein-like absorption peaks at 40 days, while the latter exhibited these peaks at 20 days. This indicated that microorganisms preferentially used benzoic acid when it was present. Additionally, fluorescence intensities of characteristic peaks tended to decrease initially and then increase, with late-stage fluorescence intensities in group 1 significantly higher than those in group 2. During the gas production period, more protein-like peaks appeared in the Sihe area than in other areas, with a lower fluorescence intensity at 40 days. This variation might be attributable to the initial coalbed water source in the experimental microbial flora from the Sihe area.[43] Previous research by various scholars has yielded comparable findings, indicating that the microbial degradation of coal byproducts involved a number of organic compounds, including aliphatics, polycyclic aromatic hydrocarbons, predominantly single-ring aromatics, and aromatic nitrogen compounds. Conversely, some researchers postulated that the microbial communities responsible for biodegrading coals do not exhibit a marked preference for either aliphatic or aromatic carbon sources.[44]

3.4. Comparison of Fluorescence Integrals and Fluorescence Indices in Each Region of the Fluorescence Map for Different Rank Coals at the Time of Peak Gas Production. *3.4.1. Comparison of Fluorescence Integrals in Each Region of the Fluorescence Profiles of Different Rank Coals during Gas Production.* The fluorescence integrals of coal samples in different periods of gas production are shown in Figure 8, where Φ1−Φ5 represent the fluorescence integrals of regions I−V, respectively, reflecting the organic matter concentration in the corresponding regions. Notably, Φ5 (corresponding to humic acids) exhibited the most distinct changes from the rapid period to the peak period. Furthermore, during the peak gas production period, the fluorescence integral of the coal samples from the Sihe group (S) notably decreased. This decrease was negatively correlated with the increase in gas production during this period, further indicating the essential influence of humic acids on the gas production process. Previous studies have shown similar results. The position of the fluorescence peak for the intermediate product in the biogas gasification process changed as the gasification time elapsed. Additionally, the fluorescence integrals of the intermediate decreased over time.

https://doi.org/10.1021/acsomega.4c09883
ACS Omega 2025, 10, 16169−16183

3.4.2. Changes in Fluorescence Intensity and Fluorescence Index during the Biogenic Gas Production with Different Rank Coals. The fluorescence index is a quantitative parameter that describes the fluorescence signal characteristics of a sample and is often used to characterize the relative contents of different components in the sample.

$$\mathbf{FI} = \frac{I_{370,450}}{I_{370,500}} \quad (4)$$

The Fluorescence Index (FI) indicated that humic acid was primarily imported from exogenous sources, while FI > 1.9 indicated endogenous humic acid production.[45] As shown in Figure 9, most samples in each group exhibited a fluorescence

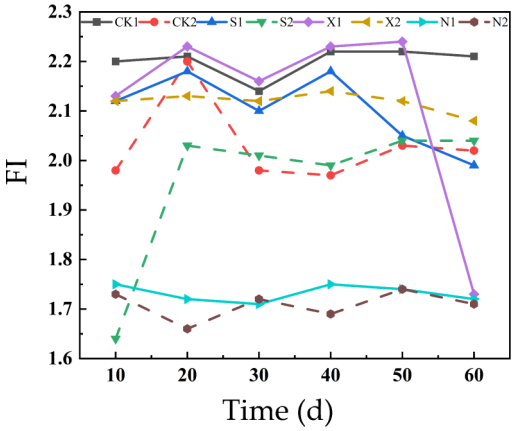

Figure 9. Variation curves of the fluorescence index during biogenic gas formation with different rank coals.

index of >1.6, excluding N2 and N1, which were >1.9. This indicated that humic acid was primarily derived from biogenic sources during biogas production. The negative correlation between humic aromaticity and FI, with higher values of FI indicating lower aromaticity and fewer aromatic ring structures in humic substances, suggested the presence of a large number of microbial metabolites in the liquid-phase system. The formula for calculating FI is as follows:

Three-dimensional fluorescence spectroscopy analysis showed that major changes in fluorescence peaks occurred during the rapid gas production period. Samples from the Sihe region exhibited levels higher than those from other regions during the peak gas production period. Notably, the fluorescence peaks exhibited sudden changes, with the characteristic absorption peak of the humic acid-like material transitioning from 1 to 2, and the intensity of the fluorescence peak decreased. Generally, these findings are in agreement with the gas production and UV analysis results, indicating that humic acid-like substances played a crucial role during the gas production period. Reflectivity and the coal-rock fraction of the coal samples affected the construction of the solution system for microbial coal gas production owing to the excellent development of pore spaces in middle- and upper-grade coals, facilitating nutrient transport by microorganisms. Future research should investigate whether using native microbes to produce gas from local coal is more efficient and explore the optimal ratios.

4. CONCLUSIONS

In the present work, taking three different rank coals as substrates, the effect of benzoic acid on biogas with enriched methanogenic microbes was investigated, combining UV−vis and 3D fluorescence spectra. The main findings are listed as follows:

All three coal samples can be utilized to produce gas with domesticated microbial flora. Distinct differences existed in the gas production effects and spectroscopic properties of the liquid-phase compositions among different rank coals. Adding benzoic acid into the culture media obviously enhanced biogas production with coal.

The UV spectra exhibited a gradual increase in the molecular weight of DOM, aromatization, and an increased number of aromatic ring substituents with hydrogen- and oxygen-containing functional groups during the gas formation process.

Fluorescence spectra revealed changes in protein-like substances (humic acid, tyrosine, and tryptophan) during the gas production process, suggesting that humic acid substances in coal were utilized by microorganisms, participating in gas production.

The FI for most samples was >1.9, indicating the presence of a large number of microbial metabolites produced during biogas production with coal.

AUTHOR INFORMATION

Corresponding Author

Huan He − *Key Laboratory of Coal Processing and Efficient Utilization of Ministry of Education, School of Chemical Engineering and Technology, China University of Mining and Technology, Xuzhou 221116, China*; Phone: 86-516-83881059; Email: hehuan6819@cumt.edu.cn

Authors

Guoqin Wei − *Institute of Resource and Environment, Henan Polytechnic University, Jiaozuo 454000, China; State Key Laboratory of Coal and CBM Co-Mining, Shanxi Jinneng Group Co., Ltd., Jincheng 048000, China; Yi'an Lanyan Coal and Coalbed Methane Co-Mining Technology Co. Ltd., Taiyuan 030031, China*; orcid.org/0009-0000-2915-1134

Dangyu Song − *Institute of Resource and Environment, Henan Polytechnic University, Jiaozuo 454000, China*; orcid.org/0000-0001-5906-0161

Xianbo Su − *Institute of Resource and Environment, Henan Polytechnic University, Jiaozuo 454000, China*

Daping Xia − *Institute of Resource and Environment, Henan Polytechnic University, Jiaozuo 454000, China*

Yunbo Li − *Institute of Resource and Environment, Henan Polytechnic University, Jiaozuo 454000, China*; orcid.org/0000-0001-7522-8198

Yu Qiao − *Institute of Resource and Environment, Henan Polytechnic University, Jiaozuo 454000, China*; orcid.org/0000-0003-0708-7500

Complete contact information is available at: https://pubs.acs.org/10.1021/acsomega.4c09883

Author Contributions

G.W. designed the experiment and wrote the manuscript. X.S. and D.X. organized and analyzed the data. H.H. and D.S.

https://doi.org/10.1021/acsomega.4c09883
ACS Omega 2025, 10, 16169−16183

provided the experimental equipment, and Y.L. and Y.Q. provided technical support.

Notes

The authors declare no competing financial interest.

■ ACKNOWLEDGMENTS

The authors acknowledge funding from the National Natural Science Foundation of China (U2003104, 42272210, 42172187), the Fundamental Research Funds for the Universities of Henan Province (NSFRF220433), the National Key Research and Development Program of China (2023YFF1306003), the Coalbed Methane Joint Research Fund of Shanxi Province (2016012012), and the Major Science and Technology Project in Shanxi Province (20191102001).

■ REFERENCES

(1) Tao, S.; Chen, S.; Pan, Z. Current status, challenges, and policy suggestions for coalbed methane industry development in China: A review. *Energy Sci. Eng.* **2019**, *7*, 1059−1074.
(2) Perendeci, N. A.; Yılmaz, V.; Ertit Taştan, B.; Gökgöl, S.; Fardinpoor, M.; Namlı, A.; Steyer, J. P. Correlations between biochemical composition and biogas production during anaerobic digestion of microalgae and cyanobacteria isolated from different sources of Turkey. *Bioresour. Technol.* **2019**, *281*, 209−216.
(3) Han, Q.; Guo, H.; Zhang, J.; Huang, Z.; Urynowicz, M. A.; Ali, M. I. Methane Generation from Anthracite by Fungi and Methanogen Mixed Flora Enriched from Produced Water Associated with the Qinshui Basin in China. *ACS Omega* **2021**, *6*, 31935−31944.
(4) Wang, A.; Shao, P. Effects of Organic Maceral on Biogenic Coalbed Gas Generation from Bituminous Coal. *ACS Omega* **2022**, *7* (21), 18139−18145.
(5) Postawa, K.; Szczygieł, J.; Kułażyński, M. Innovations in anaerobic digestion: A model-based study. *Biotechnol. Biofuels* **2021**, *14*, 19.
(6) Tao, S.; Pan, Z.; Tang, S.; Chen, S. Current status and geological conditions for the applicability of CBM drilling technologies in China: A review. *Int. J. Coal Geol.* **2019**, *202*, 95−108.
(7) Omar, B.; El-Gammal, M.; Abou-Shanab, R.; Fotidis, I. A.; Angelidaki, I.; Zhang, Y. Biogas upgrading and biochemical production from gas fermentation: Impact of microbial community and gas composition. *Bioresour. Technol.* **2019**, *286*, 121413.
(8) Chen, L.; Wang, B.-Y.; Tai, C.; Guan, J.-D.; Zhao, H.; Wang, M.-L.; Han, Z.-Y. Composition and conversion of intermediate products in the process of anthracite gasification by microorganism. *China Coal Soc.* **2016**.
(9) Liu, J.; Wang, B.; Tai, C.; Wu, L.; Zhao, H.; Guan, J.; Chen, L. An Effective Method to Detect Volatile Intermediates Generated in the Bioconversion of Coal to Methane by Gas Chromatography-Mass Spectrometry after In-Situ Extraction Using Headspace Solid-Phase Micro-Extraction under Strict Anaerobic Conditions. *PLoS One* **2016**, *11*, No. e0163949.
(10) Robbins, S. J.; Evans, P. N.; Esterle, J. S.; Golding, S. D.; Tyson, G. W. The effect of coal rank on biogenic methane potential and microbial composition. *Int. J. Coal Geol.* **2016**, *154*, 205−212.
(11) Jones, E. J. P.; Harris, S. H.; Barnhart, E. P.; Orem, W. H.; Clark, A. C.; Corum, M. D.; Kirshtein, J. D.; Varonka, M. S.; Voytek, M. A. The effect of coal bed dewatering and partial oxidation on biogenic methane potential. *Int. J. Coal Geol.* **2013**, *115*, 54−63.
(12) Schnürer, A. Biogas production: Microbiology and technology. *Adv. Biochem. Eng. Biotechnol.* **2016**, *156*, 195−234.
(13) Ma, L. T.; Liu, Y. Y.; Dong, L. C.; Wang, Y. X. Effects of Benzoic Acid on Lignite Biomethanation. *Coal Convers.* **2019**, *42*, 73−77.
(14) Salama, Y.; Chennaoui, M.; Sylla, A.; Mountadar, M.; Rihani, M.; Assobhei, O. Characterization, structure, and function of extracellular polymeric substances (EPS) of microbial biofilm in biological wastewater treatment systems: A review. *Desalin. Water Treat.* **2016**, *57*, 16220−16237.
(15) Sherma, J.; Rabel, F. Review of advances in planar chromatography-mass spectrometry published in the period 2015−2019. *J. Liq. Chromatogr. Relat. Technol.* **2020**, *43*, 394−412.
(16) Wang, K.; Ren, H.; Yuan, S.; Jiang, X.; Wang, P. Exploring the diversity of dissolved organic matter (DOM) properties and sources in different functional areas of a typical macrophyte - derived lake combined with optical spectroscopy and FT-ICR MS analysis. *J. Environ. Sci.* **2025**, *147*, 462−473.
(17) Wang, B.; Tai, C.; Wu, L.; Chen, L.; Liu, J.; Hu, B.; Song, D. Methane production from lignite through the combined effects of exogenous aerobic and anaerobic microflora. *Int. J. Coal Geol.* **2017**, *173*, 84−93.
(18) Sardana, A.; Cottrell, B.; Soulsby, D.; Aziz, T. N. Dissolved organic matter processing and photoreactivity in a wastewater treatment constructed wetland. *Sci. Total Environ.* **2019**, *648*, 923−934.
(19) Xia, D.; Gu, P.; Chen, Z.; Chen, L.; Wei, G.; Wang, Z.; Cheng, S.; Zhang, Y. Control Mechanism of Microbial Degradation on the Physical Properties of a Coal Reservoir. *Processes* **2023**, *11*, 1347.
(20) Yazdani, M.; Ebrahimi-Nik, M.; Heidari, A.; Abbaspour-Fard, M. H. Improvement of biogas production from slaughterhouse wastewater using biosynthesized iron nanoparticles from water treatment sludge. *Renewable Energy* **2019**, *135*, 496−501.
(21) Aiken, G.Fluorescence and dissolved organic matter: A chemist's perspective*Aquatic Organic Matter Fluorescence*Cambridge University Press201435−74
(22) Wang, S.; Li, Y.; Xiao, K.; Huang, X. Fluorescence excitation-emission matrix as a novel indicator of assimilable organic carbon in wastewater: Implication from a coal chemical wastewater study. *Sci. Total Environ.* **2022**, *804*, 150144.
(23) Rodríguez, F. J.; Schlenger, P.; García-Valverde, M. A comprehensive structural evaluation of humic substances using several fluorescence techniques before and after ozonation. Part I: Structural characterization of humic substances. *Sci. Total Environ.* **2014**, *476*, 718−730.
(24) Paritosh, K.; Yadav, M.; Chawade, A.; Sahoo, D.; Kesharwani, N.; Pareek, N.; Vivekanand, V. Additives as a support structure for specific biochemical activity boosts in anaerobic digestion: A review. *Front. Energy Res.* **2020**, *8*, 88.
(25) Tao, S.; Chen, S.; Tang, D. Material composition, pore structure and adsorption capacity of low-rank coals around the first coalification jump: A case of eastern Junggar Basin, China. *Fuel* **2018**, *211*, 804−815.
(26) Zabranska, J.; Pokorna, D. Bioconversion of carbon dioxide to methane using hydrogen and hydrogenotrophic methanogens. *Biotechnol. Adv.* **2018**, *36*, 707−720.
(27) Whiticar, M. J. Carbon and hydrogen isotope systematics of bacterial formation and oxidation of methane. *Chem. Geol.* **1999**, *161*, 291−314.
(28) Sikarwar, V. S.; Zhao, M.; Fennell, P. S.; Shah, N.; Anthony, E. J. Progress in biofuel production from gasification. *Prog. Energy Combust. Sci.* **2017**, *61*, 189−248.
(29) Strapoc, D.; Mastalerz, M.; Dawson, K.; Macalady, J.; Callaghan, A. V.; Wawrik, B.; Turich, C.; Ashby, M. Biogeochemistry of microbial coal-bed methane. *Annu. Rev. Earth Planet. Sci.* **2011**, *39*, 617−656.
(30) Wawrik, B.; Mendivelso, M.; Parisi, V. A.; Suflita, J. M.; Davidova, I. A.; Marks, C. R.; van Nostrand, J. D.; Liang, Y.; Zhou, J.; Huizinga, B. J.; et al. Field and laboratory studies on the bioconversion of coal to methane in the San Juan Basin. *FEMS Microbiol. Ecol.* **2012**, *81*, 26−42.
(31) Fallgren, P. H.; Jin, S.; Zeng, C.; Ren, Z.; Lu, A.; Colberg, P. J. Comparison of coal rank for enhanced biogenic natural gas production. *Int. J. Coal Geol.* **2013**, *115*, 92−96.
(32) Harris, S. H.; Smith, R. L.; Barker, C. E. Microbial and chemical factors influencing methane production in laboratory incubations of low-rank subsurface coals. *Int. J. Coal Geol.* **2008**, *76*, 46−51.
(33) Johnson, C. W.; Beckham, G. T. Aromatic catabolic pathway selection for optimal production of pyruvate and lactate from lignin. *Metab. Eng.* **2015**, *28*, 240−247.
(34) Szubert, A.; Kapusta, P.; Matyasik, I. Parameters and methods for evaluation of lignite processing method into biogas. *Physicochem. Probl. Miner. Process.* **2020**, *56*, 396−405.

https://doi.org/10.1021/acsomega.4c09883
ACS Omega 2025, 10, 16169−16183

(35) El-Nahhal, I.; Redon, R.; Raynaud, M.; El-Nahhal, Y.; Mounier, S. Characterization of the fate and changes of post-irradiance fluorescence signal of filtered anthropogenic effluent dissolved organic matter from wastewater treatment plant in the coastal zone of Gapeau river. *Environ. Sci. Pollut. Res.* **2020**, *27*, 23141−23158.
(36) Aleku, G. A.; Roberts, G. W.; Titchiner, G. R.; Leys, D. Synthetic enzyme-catalyzed CO_2 fixation reactions. *ChemSuschem* **2021**, *14*, 1781−1804.
(37) Leng, R. A. Interactions between microbial consortia in biofilms: A paradigm shift in rumen microbial ecology and enteric methane mitigation. *Anim. Prod. Sci.* **2014**, *54*, 519−543.
(38) Kulikova, N. A.; Perminova, I. V. Interactions between humic substances and microorganisms and their implications for nature-like bioremediation technologies. *Molecules* **2021**, *26*, 2706.
(39) Bejaoui, S.; Mercier, X.; Desgroux, P.; Therssen, E. Laser induced fluorescence spectroscopy of aromatic species produced in atmospheric sooting flames using UV and visible excitation wavelengths. *Combust. Flame* **2014**, *161*, 2479−2491.
(40) Murphy, K. R.; Hambly, A.; Singh, S.; Henderson, R. K.; Baker, A.; Stuetz, R.; Khan, S. J. Organic matter fluorescence in municipal water recycling schemes: Toward a unified PARAFAC model. *Environ. Sci. Technol.* **2011**, *45*, 2909−2916.
(41) Zhang, Z.; Guo, L.; Wang, Y.; Li, F.; Zhao, Y.; Gao, M.; She, Z. Degradation and transformation of extracellular polymeric substances (EPS) and dissolved organic matters (DOM) during two-stage anaerobic digestion with waste sludge. *Int. J. Hydrogen Energy* **2017**, *42*, 9619−9629.
(42) Huang, Z.; Urynowicz, M. A.; Colberg, P. J. Stimulation of biogenic methane generation in coal samples following chemical treatment with potassium permanganate. *Fuel* **2013**, *111*, 813−819.
(43) Zhang, L.; Liu, H.; Wang, Y.; Peng, Y. Compositional characteristics of dissolved organic matter during coal liquefaction wastewater treatment and its environmental implications. *Sci. Total Environ.* **2020**, *704*, 135409.
(44) Wu, L.; Li, H.; Cao, B.; Zhao, T.; Wang, Z. Study on gas characterization and fluorescence characteristics of intermediates in biogenic gas production from lignite by ultrasound assisted hydrogen peroxide pretreatment. *Arab. J. Geosci.* **2021**, *14*, 269.
(45) Heo, J.; Yoon, Y.; Kim, D. H.; Lee, H.; Lee, D.; Her, N. A new fluorescence index with a fluorescence excitation-emission matrix for dissolved organic matter (DOM) characterization. *Desalin. Water Treat.* **2016**, *57*, 20270−20282.

https://doi.org/10.1021/acsomega.4c09883
ACS Omega 2025, 10, 16169−16183